Semiconductor surface emitting lasers for photon pairs generation

Luc R. Vanbever,[1] Evgueni Karpov,[1] and Krassimir Panajotov[2]
[1]*Quantum Information and Communication, Ecole Polytechnique de Bruxelles, CP 165, Universite libre de Bruxelles, 1050 Bruxelles, Belgium*
[2]*Brussels Photonic Team, Department of Applied Physics and Photonics (B-PHOT), Vrije Universiteit Brussels, Pleinlaan 2, 1050 Brussels, Belgium*

(Received 31 May 2017; accepted 4 August 2017; published online 15 September 2017)

We study the feasibility of generating photon pairs in a resonant Vertical-Cavity Surface-Emitting Laser (VCSEL) as a result of a third-order non-linear, four wave mixing interaction. We focus on degenerate four wave mixing in the spontaneous regime where two pump photons are annihilated to create a pair of signal and idler photons. Using the methods of quantum optics, we calculate the two-photon production rate, the spectrum of the generated photons, and the signal-idler cross-correlations. We highlight how the dispersion of the medium in the VCSEL cavity (a regular GaAs configuration) significantly diminishes the two-photon production rate. Based on our results, we enumerate the characteristics of a VCSEL that would be suitable for photon pair generation. *Published by AIP Publishing.* [http://dx.doi.org/10.1063/1.4985641]

The second quantum revolution that we have been witnessing for the past few decades opens new horizons for fast computation, communication, and cryptography. Heralded single-photon sources enable optical implementations of rapidly developing quantum technologies and make possible the realization of these revolutionary ideas. Like previously for electronics, one of the key issues for quantum optical technologies is scalability achieved by integration of optical components. This makes small-size photon sources such as Vertical-Cavity Surface-Emitting Lasers (VCSELs) highly important for future development. Here, we present our study of the possibility of using VCSELs for photon pair generation based on third-order non-linear effects in semiconductor materials. With the help of the methods of quantum optics, we calculated relevant parameters of photon pair generation including the two-photon production rate, their spectrum of emitted photons, and the cross-correlations between the photons in each pair. Based on our results, we specified the requirements for the design of VCSELs capable of providing a sufficiently high photon-pair generation rate.

I. INTRODUCTION

Entangled and single photon sources are a key ingredient in a wide range of applications of quantum information, including quantum computation,[1,2] communication,[3,4] cryptography,[5–7] and quantum metrology.[8] They are based on nonlinear optical effects, among which one can mention parametric down conversion[9,10] and quantum dots exploiting the Purcell effect.[11,12] Modern quantum technologies are trying to achieve scalability by using integrated photonic quantum circuits on chip, for example, for boson sampling.[13] The photon sources suitable for on-chip integration are at hand for future development.

Cost-effectiveness and ubiquity of current VCSELs[14–16] are the main drivers for this analysis. Considering their current size and manufacturing process, VCSEL devices appear to be easily scalable.[17–20] Massive arrays of VCSEL sources generating entangled photons would result in a number of applications in modern quantum technologies. Furthermore, the mature VCSEL technology gives the advantage of developing monolithic, electrically injected photon pair sources.

The second order non-linear susceptibility $\chi^{(2)}$ value in a VCSEL does not allow for parametric down conversion, and we are taking advantage of the relatively high value of the third-order non-linearity $\chi^{(3)}$. We analyze the feasibility of producing photon pairs by four wave mixing within a resonant semiconductor VCSEL cavity. Degenerate four wave mixing allows the generation of a pair of photons whose frequencies are equidistant from the pump frequency, potentially allowing easy separation of the generated photons by filtering.[21]

The efficient conversion of two pump photons into a signal and an idler photon by degenerate four wave mixing requires that the non-linear material allows both conservation of energy ($2\omega_{pump} = \omega_{signal} + \omega_{idler}$) and conservation of momentum ($2k_{pump} = k_{signal} + k_{idler}$), also referred to as phase matching. As was already emphasized,[22,23] highly dispersive materials hinder such conservation, and we need to take into account the impact of the dispersion in our study. The refractive index of the material used in VCSELs is not constant, having a wavelength-dependent value; therefore, two waves that fulfill the phase matching criteria ($2k_{pump} = k_{signal} + k_{idler}$) will not straightforwardly allow the conservation of energy ($2\omega_{pump} \neq \omega_{signal} + \omega_{idler}$). Expressed in angular frequency, this difference between the energy of the two pump photons ($2\omega_{pump}$) and the sum of the energies of the (possibly) emitted signal and idler photons ($\omega_{signal} + \omega_{idler}$) is called the spectral walk-off. The spectral walk-off will affect the spectrum of the emitted photons, strongly reducing the number of emitted photon pairs when the difference between the refractive index of the signal and idler photons becomes high. In the case of our VCSEL, the refractive index grows monotonically with the frequency. As a result, the spectrum of the emitted photons will be considerably narrowed around the

pump angular frequency. Our analysis shows that the efficiency of our photon pair production scheme will depend on the technical capability to limit the spectral walk-off, that is, to compensate the dispersion of the material.

To evaluate the feasibility of generating photon pairs by degenerate four wave mixing from a VCSEL, we estimate the two-photon production rate and two other parameters that characterize photon sources: the frequency spectrum of the photon pairs and their cross-correlation.

We make a series of simplifying assumptions to perform this evaluation. We emphasize two of those assumptions:

- We consider only the physical effect of interest in this article: degenerate four wave mixing. The variety of physical effects that "disturb" the two-photon production is neglected in our calculation. Chen *et al.* enumerated[23] the non-linear physical effects that can occur in the non-linear material (for instance Raman scattering).
- The VCSEL cavity is designed to be resonant for the pump, signal, and idler frequencies.

Future technical designs of the VCSEL sources aimed at generating photon pairs should comply with those assumptions. Other assumptions are made and explained prior to the calculations in each section.

To calculate the two-photon production rate, the frequency spectrum of the emitted photons, and their cross-correlation for our VCSEL cavity, we follow the approach presented by Herzog *et al.*,[24] where those three values are calculated for a $\chi^{(2)}$ down-conversion process using an Optical Parametric Oscillator. We start in Sec. II by defining the expressions for the electric field operators applicable to our environment and use a perturbative treatment to derive expressions for the two-photon wave function. We then use those expressions to calculate the two-photon production rate in Sec. III, the output spectrum of the signal wave in Sec. IV, and the signal-idler cross-correlation in Sec. V. We present a discussion of the results of our analysis and a conclusion in Sec. VI.

II. THE TWO-PHOTON WAVE FUNCTION

A. Expressions for the fields

In our calculations, electric fields in the cavity will be split into four components identified by the $^{(+)}$ or $^{(-)}$ symbol that refers to the component of the field oscillating as $e^{-i\omega_p t}$ or as $e^{+i\omega_p t}$, respectively, and also by indices $+x$ or $-x$, indicating whether the field wave travels in the positive or negative direction, respectively. The pump, signal, and idler optical fields in the cavity are assumed to be linearly co-polarized.[25] The resonant VCSEL cavity is assumed to be pumped by a classical pump field

$$\begin{aligned} E_p(x,t) &= E_p^{(+)}(x,t) + E_p^{(-)}(x,t) \\ &= E_{p,+x}^{(+)}(x,t) + E_{p,+x}^{(-)}(x,t) \\ &\quad + E_{p,-x}^{(+)}(x,t) + E_{p,-x}^{(-)}(x,t), \end{aligned}$$

where, for example, the component of the pump field travelling in the $+x$ direction[24] and oscillating as $e^{-i\omega_p t}$ is

$$E_{p,+x}^{(+)}(x,t) = E_p e^{i[k_p(\omega_p)x - \omega_p t]}. \tag{1}$$

In what follows, we will omit the $+x$ index, indicating the travelling direction because in our calculations, we will only make use of the components of the fields travelling in the positive x direction. From now on, the $+x$ index must be assumed for all resonant fields: pump, signal, and idler intracavity fields. The resonant cavity is considered as lossless for the strong pump field.

To define expressions for the signal and idler field operators in the cavity, we start from the expression for the resonant field travelling in the x direction in a lossless cavity[24]

$$E^{(+)}(x,t) = \frac{1}{2}\sum_{m=1}^{\infty}\left(\frac{\hbar\omega_m}{\varepsilon_0 V}\right)^{1/2} a_m e^{i\omega_m\left(\frac{x}{c}-t\right)}. \tag{2}$$

In this expression, V is the volume of the resonant VCSEL cavity, equal to the product of A, the transverse section of the interaction volume, and L the length of the cavity, c is the speed of light in the vacuum, ε_0 is the permittivity of the vacuum. a_m is the annihilation operator corresponding to the resonant cavity mode identified by m and obeys the usual bosonic commutation relations $[a_m, a_n^\dagger] = \delta_{mn}$.

Some authors make an approximation by moving the angular frequency ω_m out of the sum.[26] In the case of our VCSEL, the resonant modes are relatively distant from each other in the frequency domain ($(\omega_{m+1} - \omega_m)/\omega_m \approx 5\%$), and we do not make the upfront simplification $\omega_m \approx \omega$ for any m (although we will make such simplification later in order to make feasible numerical estimations).

Eq. (2) is valid in the vacuum, and in order to have a correct description of the fields in our cavity, we need to take into account the refractive index $n(\omega)$ of the resonant medium.[27] The expression for the electric field in the VCSEL cavity becomes

$$E^{(+)}(x,t) = \frac{1}{2}\sum_{m=1}^{\infty}\left(\frac{\hbar\omega_m}{\varepsilon_0 V n^2(\omega_m)}\right)^{1/2} a_m e^{i\omega_m\left(\frac{x}{c}n(\omega_m)-t\right)}. \tag{3}$$

To account for the losses in the cavity, we have to replace the annihilation operator a_m by a time-dependent operator $a_m(t)$ which can be expressed in terms of its Fourier components as[22,24,26]

$$a_m(t) = \frac{1}{\sqrt{2\pi}}\int_{-\infty}^{+\infty} d\Omega a(\omega_m + \Omega)\frac{\sqrt{\gamma_s}}{\frac{\gamma_s}{2} + i\Omega}e^{-i\Omega t},$$

where γ_s is the damping rate of the signal wave, which reflects the photon emission out of the one-side cavity. We assume that the damping rate γ_s (γ_i) has the same value for all signal (idler) waves in the cavity. We note that $a_m(t)$ has no dimension and $a(\omega)$ has the dimension of square root of time ($s^{1/2}$).

We denote the resonant pump, signal, and idler modes by the indices m_p, m_s, and m_i, respectively, and the corresponding signal and idler angular frequencies by ω_{m_s} and ω_{m_i}, respectively.

After replacement of a_m by $a_m(t)$ in Eq. (3), we arrive at the following expressions for the signal and idler fields travelling in the positive x direction $E^{(+)}_{s/i}(x,t)$ in the lossy VCSEL cavity[24]

$$E^{(+)}_{s/i}(x,t) = \frac{1}{2}\sum_{m_{s/i}=1}^{\infty}\left(\frac{\hbar\omega_{m_{s/i}}}{2\pi\varepsilon_0 V n^2(\omega_{m_{s/i}})}\right)^{1/2}\int_{-\infty}^{+\infty} d\Omega a(\omega_{m_{s/i}}+\Omega) \times \frac{\sqrt{\gamma_{s/i}}}{\frac{\gamma_{s/i}}{2}+i\Omega} e^{i\left[k_{s/i}(\Omega)x-(\omega_{m_{s/i}}+\Omega)t\right]}, \quad (4)$$

where the x-component $k_{s/i}(\Omega)$ of the wave vector of the mode $m_{s/i}$ is

$$k_{s/i}(\Omega) = 2\pi m_{s/i}/L = (\omega_{m_{s/i}}+\Omega)n(\omega_{m_{s/i}}+\Omega)/c\,. \quad (5)$$

The non-constant factor $n(\omega_{m_{s/i}}+\Omega)$ in Eq. (5) reflects the dispersion of the material and, as will be seen later in this text, will induce a spectral walk-off between (potentially) created photon pairs. In turn, the induced spectral walk-off will strongly affect the two-photon production rate.

We note that although the VCSEL cavity has a layered structure, we do not take into account differences between the various layers. The above signal and idler field expressions assume that the cavity is homogeneous from the refractive index viewpoint.

The angular frequencies of the fields coming out of the cavity are assumed to be in the neighborhood of the pump angular frequency ω_p, and we use the following expression for the signal and idler outside fields

$$E^{(+)}_{Out_{s/i}}(x,t) = \left(\frac{\hbar\omega_p}{2\varepsilon_0 cA}\right)^{1/2}\int_{-\infty}^{+\infty}\frac{d\Omega}{\sqrt{2\pi}} \times a_{s/i}(\omega_p+\Omega)e^{i\left[(\omega_p+\Omega)(\frac{x}{c}-t)\right]}, \quad (6)$$

where A is the transverse cross-section of the wave.[24] Equation (6) is established by first defining the expression of the electromagnetic field in a finite volume and then taking the continuum limit by extending the quantization length to infinity. The lower limit of integration is subsequently extended to minus infinity using the fact that $\omega_p \gg 1$, that is, the bandwidths of the fields outside the cavity are assumed to be small compared to the angular frequency ω_p.[26] The signal and idler annihilation operators introduced in Eq. (6) are defined as follows: $a_s(\omega) = a(\omega)$ for $\omega > \omega_p$ and $a_s(\omega) = 0$ for $\omega \le \omega_p$ and $a_i(\omega) = a(\omega)$ for $\omega < \omega_p$ and $a_i(\omega) = 0$ for $\omega \ge \omega_p$.

B. Expressions for the two-photon wave function

The interaction Hamiltonian describing our degenerate four wave mixing interaction has the following expression (refer to Appendix B for its derivation):

$$H_{int} = \frac{3}{2}\varepsilon_0\int_V \chi^{(3)}E_p^{(+)}E_p^{(+)}E_s^{(-)}E_i^{(-)}dV + H.c.\,, \quad (7)$$

where V is the interaction volume, $\chi^{(3)}$ is the third-order non-linear susceptibility,[22] and the signal and idler modes satisfy $m_s + m_i = 2m_p$. We define $\Delta m = m_p - m_i = m_s - m_p$. The off-diagonal terms of the third-order non-linear susceptibility tensor have been neglected,[25] and $\chi^{(3)}$ is considered as a constant parameter below.

We calculate the state $|\psi_c\rangle$ of the radiation field in the VCSEL cavity by means of first order perturbation expansion

$$|\psi_c\rangle \approx |0\rangle + \frac{1}{i\hbar}\int_0^{\Delta t} H_{int}(t)dt\,|0\rangle \approx |0\rangle + |\psi\rangle, \quad (8)$$

which defines the (non-normalized) perturbation state $|\psi\rangle$ that will be referred to as the two-photon state.

The perturbation treatment is valid when the perturbation is weak, that is, when the probability to be in the two-photon state $\langle\psi|\psi\rangle \ll 1$. Also, the cavity can safely be assumed to be in the vacuum state before each two-photon emission if the production rate is significantly lower than the cavity damping rates: $\langle\psi|\psi\rangle/\Delta t \ll \gamma_{s/i}$.[24,27]

Inserting Eqs. (1), (4), and (7) into Eq. (8) and rearranging the terms, we obtain the two-photon state $|\psi\rangle$ (here and in what follows, when integration limits are omitted, $-\infty$ to $+\infty$ must be assumed):

$$|\psi\rangle = \frac{3}{16\pi}\chi^{(3)}E_p^2\Delta t(\gamma_s\gamma_i)^{1/2}\sum_{\Delta m=1}^{m_p-1}\frac{(\omega_{m_s}\omega_{m_i})^{1/2}}{n(\omega_{m_s})n(\omega_{m_i})} \times \int d\Omega\int d\Omega'\frac{S_{si}(\Omega,\Omega')}{\left(\frac{\gamma_s}{2}-i\Omega\right)\left(\frac{\gamma_i}{2}-i\Omega'\right)} \times e^{i(\Omega+\Omega'-\Delta_{msi})\frac{\Delta t}{2}}\mathrm{sinc}\left[(\Omega+\Omega'-\Delta_{msi})\frac{\Delta t}{2}\right] \times a^\dagger(\omega_{m_s}+\Omega)a^\dagger(\omega_{m_i}+\Omega')\,|0\rangle, \quad (9)$$

where we have used the following mathematical identities:

$$\int_0^a dt\,e^{i\beta t} = \int_{-a}^0 dx\,e^{-i\beta x} = a\,e^{i\beta\frac{a}{2}}\mathrm{sinc}\left(\beta\frac{a}{2}\right)$$

and defined the mode-dependent spectral walk-off $\Delta_{msi} = 2\omega_p - \omega_{m_s} - \omega_{m_i}$, as well as the function

$$S_{si}(\Omega,\Omega') = e^{i\left(2k_p(\omega_p)-k_s(\Omega)-k_i(\Omega')\right)\frac{L}{2}} \times \mathrm{sinc}\left[\left(2k_p(\omega_p)-k_s(\Omega)-k_i(\Omega')\right)\frac{L}{2}\right]. \quad (10)$$

In this expression, ω_p and L are parameters of the function $S_{si}(\Omega,\Omega')$. The function $\mathrm{sinc}(x) = \sin(x)/x$ is the unnormalized sinc function.

III. TWO-PHOTON PRODUCTION RATE

To compute the two-photon production rate $\frac{\langle\psi|\psi\rangle}{\Delta t}$, we start from (9). By using the relation $a(\omega_{m_{s/i1}}+\Omega_1)a^\dagger(\omega_{m_{s/i2}}+\Omega_2)\,|0\rangle = \delta_{m_{s/i1},m_{s/i2}}\delta(\Omega_1-\Omega_2)\,|0\rangle$, valid for two non-overlapping modes in the frequency domain, we obtain[24]

$$\frac{\langle\psi|\psi\rangle}{\Delta t} = \left(\frac{3}{16\pi}\chi^{(3)}E_p^2\right)^2 \gamma_s\gamma_i\Delta t \sum_{\Delta m=1}^{m_p-1} \frac{\omega_{m_s}\omega_{m_i}}{n^2(\omega_{m_s})n^2(\omega_{m_i})} \times \int d\Omega \int d\Omega' \frac{|S_{si}(\Omega,\Omega')|^2}{\left[\left(\frac{\gamma_s}{2}\right)^2+\Omega^2\right]\left[\left(\frac{\gamma_i}{2}\right)^2+\Omega'^2\right]} \times \mathrm{sinc}^2\left[(\Omega+\Omega'-\Delta_{msi})\frac{\Delta t}{2}\right]. \quad (11)$$

We continue our calculations in two cases. In the first case, it is assumed that the spectral walk-off can be compensated by the VCSEL design. The second case does not rely upon such assumption.

A. Two-photon production rate if the spectral walk-off is compensated

Compensation of the spectral walk-off ($\Delta_{msi} = 0$) allows us to make the assumption of a constant free spectral range $\Delta\omega$, which we define as

$$\Delta\omega = \omega_{m_s+1} - \omega_{m_s} = \omega_{m_i-1} - \omega_{m_i}. \quad (12)$$

We start from (11) and make the assumption that, for sufficiently large Δt, the Ω' integral is dominated by the region $(\Omega+\Omega') \leqslant 2\pi/\Delta t$.[24] If $|S_{si}(\Omega,\Omega')|^2/[(\gamma_i/2)^2+\Omega'^2]$ is a slowly varying function of Ω' in this region, the latter function can be replaced by its value at $\Omega' = -\Omega$. The validity of this approximation is analyzed in Sec. 1 of Appendix D.

We then use the relation $\int_{-\infty}^{+\infty} \mathrm{sinc}^2(x)dx = \pi$ to perform the integration over Ω'. This leads to the following two-photon production rate:

$$\frac{\langle\psi|\psi\rangle}{\Delta t} = \frac{1}{2\pi}\left(\frac{3}{8}\chi^{(3)}E_p^2\right)^2 \gamma_s\gamma_i \sum_{\Delta m=1}^{m_p-1} \frac{\omega_{m_s}\omega_{m_i}}{n^2(\omega_{m_s})n^2(\omega_{m_i})} \times \int \frac{d\Omega|S_{si}(\Omega,-\Omega)|^2}{\left[\left(\frac{\gamma_s}{2}\right)^2+\Omega^2\right]\left[\left(\frac{\gamma_i}{2}\right)^2+\Omega^2\right]}. \quad (13)$$

We make a rough evaluation of this expression for the VCSEL whose parameters are described in Appendix A. In the case of this VCSEL, $\Delta m \leq 4$ as four pairs of signal-idler photon pairs are produced above the absorption band of the VCSEL. Signal photons of lower wavelengths fall in the absorption band, defined by the wavelength $\lambda \approx 0.69\mu$m.

We further assume that in the range of values of Ω where the two Lorentzians in (13) are non-zero, we can safely make the approximation $|S_{si}(\Omega,-\Omega)|^2 = 1$. This approximation is validated in Sec. 2 of Appendix D. We also make the simplifying assumption

$$\frac{\omega_{m_s}\omega_{m_i}}{n^2(\omega_{m_s})n^2(\omega_{m_i})} \approx \frac{\omega^2{}_p}{n_p^4}. \quad (14)$$

As a result, the integral is independent of the angular frequencies ω_{m_s}, ω_p, and ω_{m_i} and becomes

$$\int_{-\infty}^{+\infty} \frac{d\Omega}{\left(\left(\frac{\gamma_s}{2}\right)^2+\Omega^2\right)\left(\left(\frac{\gamma_i}{2}\right)^2+\Omega^2\right)} = \frac{8\pi}{\gamma_s\gamma_i(\gamma_s+\gamma_i)}.$$

With these approximations, the two-photon production rate is the same for all signal-idler pairs [identified by their mode indices (m_s, m_i) and the value of Δm in the sum in Eq. (13)], and the final expression of the two-photon production rate per pair of modes when the spectral walk-off is compensated is

$$\left.\frac{\langle\psi|\psi\rangle}{\Delta t}\right|_{per\ pair\ of\ modes} = \frac{1}{(\gamma_s+\gamma_i)}\left(\frac{3\chi^{(3)}\omega_p E_p^2}{4n_p^2}\right)^2. \quad (15)$$

With the values $E_p = 2\times10^4\mathrm{Vm}^{-1}$ (lower than the laser threshold value of $2.5\times10^4\mathrm{Vm}^{-1}$ in the VCSEL), $\chi^{(3)} = 1.4\times10^{-18}\,\mathrm{m}^2\mathrm{V}^{-2}$ (third-order non-linear susceptibility of the GaAs material[28]), and $\gamma_s = \gamma_i = 300\,\mathrm{GHz}$ (typical value for a VCSEL), we obtain a two-photon production rate per pair of modes:

$$\left.\frac{\langle\psi|\psi\rangle}{\Delta t}\right|_{per\ pair\ of\ modes} = 1.08\times10^{-2}\,\mathrm{s}^{-1}.$$

It is expected that the actual third-order non-linear susceptibility for the VCSEL might be significantly higher than the value of the GaAs material used in our calculation because the above $\chi^{(3)}$ value does not take into account the quantum wells present in the layered structure of the VCSEL.

Taking into account that, in our case, Δm takes four values ($\Delta m = 1,\ldots,4$) corresponding to four resonant modes above the absorption bandwidth of the VCSEL, the total two-photon production rate when the spectral walk-off is compensated amounts to $4.32\times10^{-2}\,\mathrm{s}^{-1}$.

The two-photon production rate does not directly depend on the properties (length, volume…) of the cavity.[24]

In many cases, the damping coefficients γ_s and γ_i might have different values. The production rate varies with the ratio of the two damping coefficients as depicted in Fig. 1.

B. Two-photon production rate if the spectral walk-off is not compensated

In the case where the spectral walk-off in the VCSEL cannot or can only be partially compensated ($\Delta_{msi} \neq 0$), we need to include its effect into our expressions of the two-photon production rate. Among our references, only Ref. 22 has explicitly integrated the spectral walk-off in the perturbative calculation. Expression (11) for the two-photon production rate becomes

$$\frac{\langle\psi|\psi\rangle}{\Delta t} = \frac{1}{2\pi}\left(\frac{3}{8}\chi^{(3)}E_p^2\right)^2 \gamma_s\gamma_i \sum_{\Delta m=1}^{m_p-1} \frac{\omega_{m_s}\omega_{m_i}}{n^2(\omega_{m_s})n^2(\omega_{m_i})} \times \int \frac{d\Omega|S_{si}(\Omega,\Delta_{msi}-\Omega)|^2}{\left[\left(\frac{\gamma_s}{2}\right)^2+\Omega^2\right]\left[\left(\frac{\gamma_i}{2}\right)^2+(\Delta_{msi}-\Omega)^2\right]}, \quad (16)$$

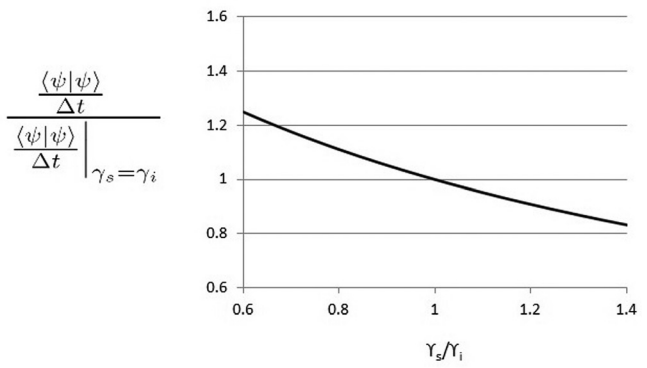

FIG. 1. Two-photon production rate $\frac{\langle\psi|\psi\rangle}{\Delta t}$ normalized to $\frac{\langle\psi|\psi\rangle}{\Delta t}|_{\gamma_s=\gamma_i}$ as a function of the ratio of signal and idler damping rates $\frac{\gamma_s}{\gamma_i}$.

which is obtained by replacing $|S_{si}(\Omega,\Omega')|^2/[(\gamma_i/2)^2+\Omega'^2]$ by its value at $\Omega'=\Delta_{msi}-\Omega$ in (11) because for sufficiently large Δt, the Ω' integral in (11) is dominated by the region $(\Omega+\Omega'-\Delta_{msi})\leqslant 2\pi/\Delta t$ (Ref. 24) and $|S_{si}(\Omega,\Omega')|^2/[(\gamma_i/2)^2+\Omega'^2]$ is a slowly varying function of Ω' in this region. The validity of this approximation is analyzed in Sec. 1 of Appendix D. We can also safely approximate the $|S_{si}(\Omega,\Delta_{msi}-\Omega)|^2$ factor by 1, as it is shown in Sec. 2 of Appendix D.

The two-photon production rate per mode calculated numerically from (16) as a function of the spectral walk-off Δ_{msi} is plotted in Fig. 2 (with the same parameters as those used in the case where there is compensation). It shows that the two-photon production rate drops dramatically when the spectral walk-off increases, in particular, if the spectral walk-off has a value larger than the cavity damping rate γ_i ($\sim$300 GHz in our case). We assume $\gamma_i=\gamma_s=\gamma$ in the following calculations of the production rates.

When the spectral walk-off is significantly larger than the cavity damping rate ($\Delta_{msi}\gg\gamma$), we can make the following approximation for the two-photon production rate:

$$\frac{\langle\psi|\psi\rangle}{\Delta t}\approx\frac{1}{\pi\Delta_{msi}^2}\left(\frac{3}{8}\chi^{(3)}E_p^2\right)^2\gamma^2\frac{\omega_p^2}{n_p^4}\int_{-\infty}^{+\infty}\frac{d\Omega}{\left(\frac{\gamma}{2}\right)^2+\Omega^2}$$

$$\approx\frac{\gamma}{2}\left(\frac{3\chi^{(3)}\omega_p E_p^2}{4\Delta_{msi}n_p^2}\right)^2, \tag{17}$$

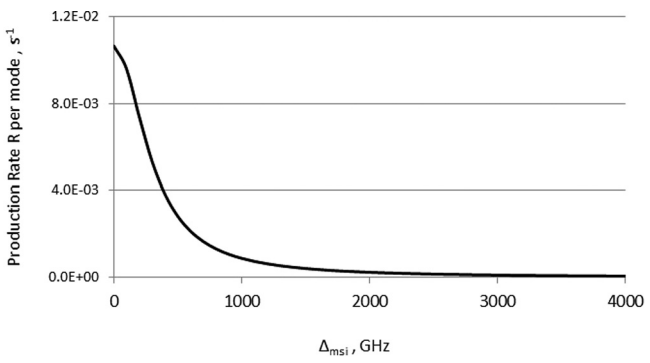

FIG. 2. Production rate per mode as a function of the spectral walk-off Δ_{msi}.

where we have made the approximation (14) and replaced the definite integral by its value $2\pi/\gamma_s$ in the last expression. Although the root cause of the dispersion is the varying value of the refractive index, making the approximation $n_p^4\approx n^2(\omega_{m_s})n^2(\omega_{m_i})$ in (14) is still acceptable to calculate an order of magnitude of the two-photon production rate. Indeed, in the case of the VCSEL considered in Appendix A, two values that might appear as strongly incompatible with the approximation are $n(\omega_{m_s}=2.69\text{PHz})=3.53$ and $n(\omega_{m_i}=1.67\text{PHz})=3.29$, which results in $n^2(\omega_{m_s})n^2(\omega_{m_i})=134.8$. We consider here that $n_p^4=133.6$ is an acceptable approximation for $n^2(\omega_{m_s})n^2(\omega_{m_i})$ for all pairs of modes m_s and m_i that intervene in our calculation. In the derivation of Eq. (17), we have only kept the first term from the sum in Eq. (16), that is, the term where $\Delta m=1$ because the value of the second term is approximately only 10% of the value of the first one in the case of the VCSEL described in Appendix A. Indeed, the product of the two Lorentzian functions in Eq. (16) is drastically decreased for $\Delta m>1$ when $\Delta_{msi}\neq 0$. It can be seen in Fig. 2 and Table II that the production rates corresponding to the modes $\Delta m=3$ ($\Delta_{msi}=31\times10^{12}\,\text{s}^{-1}$) and $\Delta m=4$ ($\Delta_{msi}=54\times10^{12}\,\text{s}^{-1}$) are even smaller in comparison to the terms $\Delta m=1$ ($\Delta_{msi}=3.4\times10^{12}\,\text{s}^{-1}$) and $\Delta m=2$ ($\Delta_{msi}=14\times10^{12}\,\text{s}^{-1}$).

Note that the production rate increases with the fourth power of the pump electric field. Table I presents the values of the two-photon production rate obtained for three values of the pump electric field, in particular, above the laser threshold. Note that the production rate $2.7\times10^5\text{s}^{-1}$ should be taken with caution as this value for the production rate might conflict with the calculation assumption $\Delta t\gg10^{-8}$s as explained in Sec. 1 of Appendix D. Increasing the power of the pump might also increase other physical effects (such as Raman scattering) that may come in addition and disturb the photon pair emission.

As the above results demonstrate, reducing the dispersion or compensating the spectral walk-off in the VCSEL cavity will be paramount to enhance the production rate of photon pairs. Different strategies can be developed for compensating the spectral walk-off, such as VCSEL waveguide dispersion management,[29–31] embedding photonic crystals in the VCSEL Distributed Bragg Reflectors and/or cavity,[32–36] utilizing optical feedback,[37] and implementing the coupled cavity-VCSEL system[38,39] where electro-optic tuning of the resonance wavelength provides additional flexibility.[40]

The production rate also increases quadratically with the material third-order non-linear susceptibility $\chi^{(3)}$. A significant

TABLE I. Two-photon production rates obtained for a couple of values of the pump electric field in the VCSEL cavity. The laser threshold value for the radiation field is 2.5×10^4V/m.

E_p, V/m	$\frac{\langle\psi\|\psi\rangle}{\Delta t}$, s^{-1} Spectral walk-off compensated	$\frac{\langle\psi\|\psi\rangle}{\Delta t}$, s^{-1} Spectral walk-off non-compensated
2×10^4	4.3×10^{-2}	8.4×10^{-5}
1×10^5	27	5.3×10^{-2}
1×10^6	2.7×10^5	5.3×10^2

increase in the production rate might be in the range of the possibilities as the value we have used $\chi^{(3)} = 1.4 \times 10^{-18}\mathrm{m}^2/\mathrm{V}^2$ is the value for the GaAs material[28] and it does not take into account the quantum wells. Utilizing the excitonic effects in quantum wells might result in an increase in the actual third-order non-linear susceptibility.[41]

IV. OUTPUT SPECTRUM

The output spectrum of the wave is given by $S(\omega) = \langle\psi|\, a^\dagger(\omega)a(\omega)\,|\psi\rangle$. We start our calculation from expression (9), and we assume that Δt is sufficiently large so that the following limit applies:[24]

$$\lim_{\Delta t\to\infty}\left(\Delta t\,\mathrm{sinc}\left[(\Omega+\Omega'-\Delta_{msi})\,\frac{\Delta t}{2}\right]\right) = 2\pi\delta(\Omega+\Omega'-\Delta_{msi})\,. \tag{18}$$

We further assume that the free spectral range, denoted as $\Delta\omega$, is constant (no dispersion, that is $\Delta_{msi}=0$), and we write $\omega_{m_s} = \omega_p + \Delta m\Delta\omega$ and $\omega_{m_i} = \omega_p - \Delta m\Delta\omega$. Then, the Dirac delta function in (18) leads to $\Omega' = -\Omega$.

At the limit of infinite Δt, the two-photon wave function (9) may then be written under the (time-independent) alternative form

$$|\psi\rangle = \frac{3}{8}\chi^{(3)}E_p^2(\gamma_s\gamma_i)^{1/2}\sum_{\Delta m=1}^{m_p-1}\frac{(\omega_{m_s}\omega_{m_i})^{1/2}}{n(\omega_{m_s})n(\omega_{m_i})} \times\int d\Omega\,\frac{S_{si}(\Omega,-\Omega)}{\left(\frac{\gamma_s}{2}-i\Omega\right)\left(\frac{\gamma_i}{2}+i\Omega\right)}\times a^\dagger(\omega_p+\Delta m\Delta\omega+\Omega) \times a^\dagger(\omega_p-\Delta m\Delta\omega-\Omega)\,|0\rangle. \tag{19}$$

Under this simplified form, the two-photon wave function cannot easily be normalized as a Dirac delta function $\delta(0)$ would intervene in the normalization calculation (also see note 26 in Herzog *et al.*[24]). This divergence in the normalization constant results from the limit that we have taken in (18). This is not an issue in our context as we are not seeking absolute values (we know the production rate), and we have written Eq. (19) in order to find out the shape of the output spectrum. We calculate

$$a(\omega)\,|\psi\rangle \propto \sum_{\Delta m=1}^{m_p-1}\frac{(\omega_{m_s}\omega_{m_i})^{1/2}}{n(\omega_{m_s})n(\omega_{m_i})}\int d\Omega\,\frac{S_{si}(\Omega,-\Omega)}{\left(\frac{\gamma_s}{2}-i\Omega\right)\left(\frac{\gamma_i}{2}+i\Omega\right)} \times a(\omega)\,a^\dagger(\omega_p+\Delta m\Delta\omega+\Omega) \times a^\dagger(\omega_p-\Delta m\Delta\omega-\Omega)\,|0\rangle$$

and we obtain the spectrum in the form

$$S(\omega)\propto\sum_{|j|=+1}^{+4}\frac{\omega_{m_p+j}\omega_{m_p-j}}{n^2(\omega_{m_p+j})n^2(\omega_{m_p-j})}\times\frac{|S_{si}(\omega-\omega_p-j\Delta\omega,\omega-\omega_p-j\Delta\omega)|^2}{\left[\left(\frac{\gamma_s}{2}\right)^2+(\omega-\omega_p-j\Delta\omega)^2\right]\left[\left(\frac{\gamma_i}{2}\right)^2+(\omega-\omega_p-j\Delta\omega)^2\right]}, \tag{20}$$

where we have used an index $j=-4,..,+4$, $j\neq 0$ that takes into account that photons with angular frequencies higher than ω_{m_p-4} are absorbed. If we take into account the spectral walk-off ($\Delta_{msi}\neq 0$), the output spectrum would be proportional to the integrand in Eq. (16). The output spectrum is depicted in Fig. 3. It is a frequency comb, as already described in other articles.[22,23]

The number of "teeth" of the comb is limited by the absorption band of the VCSEL so that our comb has only four coupled "teeth" at each side of the pump frequency, which is significantly less than that in other cases considered in the literature.[23] If the spectral walk-off is not compensated, the "amplitude" of the "teeth" decreases significantly with increasing Δm (that is, when the "teeth" gets further away from the central pump frequency).[22]

We noticed that some authors[24] use different steps and perform the calculation of the output spectrum with the help of the Fourier transform of the first order correlation function. Our result is consistent with other articles.[22,23]

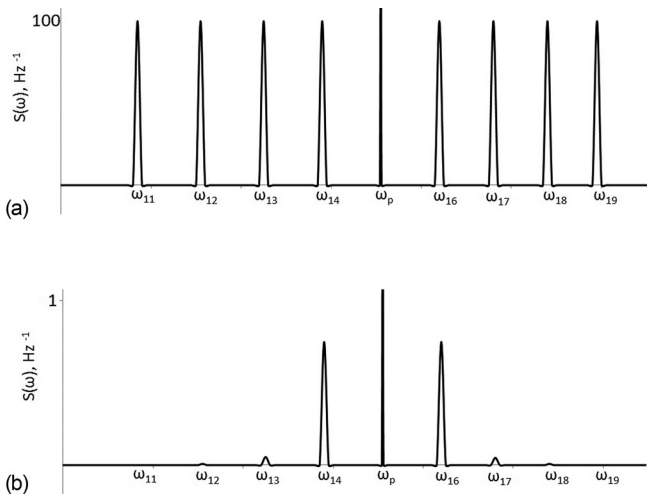

FIG. 3. Normalized signal-idler output spectra $S(\omega)$ as a function of the idler, pump, and signal angular frequencies. The values for the angular frequencies ω_{m_s} and ω_{m_i} are provided in Appendix A for $m_s = 16,\ldots,19$ and $m_i = 11,\ldots,14$. The pump angular frequency is $\omega_p = 2.2\times10^{15}\,\mathrm{s}^{-1}$. For clarity, the width of the Lorentzians represented on the graphs is larger than $\gamma = 300\,\mathrm{GHz}$ used in our calculations; (a) spectrum for $\Delta_{msi}=0$ and (b) spectrum for $\Delta_{msi}\neq 0$.

V. SIGNAL-IDLER CROSS-CORRELATION

The signal-idler cross-correlation function is defined[24] as

$$G_{IS}^{(2)} = \langle\psi| E_{Out_i}^{(-)}(x,t)\, E_{Out_s}^{(-)}(x,t+\tau) \times E_{Out_s}^{(+)}(x,t+\tau)\, E_{Out_i}^{(+)}(x,t)\,|\psi\rangle.$$

Physically, the cross-correlation function is proportional to the coincidence rate, that is, the rate of detection, at the output of the cavity, of an idler photon at time t and a signal photon at time $t+\tau$.

We perform the calculation in the case where the spectral walk-off is compensated. We start with the calculation of the state $E_{Out_s}^{(+)}(x,t+\tau)\, E_{Out_i}^{(+)}(x,t)\,|\psi\rangle$ using Eq. (19) for the two-photon wave function $|\psi\rangle$ and Eq. (6) for the signal and idler field operators in the free field[24]

$$\begin{aligned} &E_{Out_s}^{(+)}(x,t+\tau)\, E_{Out_i}^{(+)}(x,t)\,|\psi\rangle \\ &= \left[\left(\frac{\hbar\omega_p}{2\varepsilon_0 cA}\right)^{1/2}\int\frac{d\Omega'}{\sqrt{2\pi}} a_s(\omega_p+\Omega') e^{i\left[(\omega_p+\Omega')(x/c-t-\tau)\right]}\right] \\ &\times\left[\left(\frac{\hbar\omega_p}{2\varepsilon_0 cA}\right)^{1/2}\int\frac{d\Omega''}{\sqrt{2\pi}} a_i(\omega_p+\Omega'') e^{i\left[(\omega_p+\Omega'')(x/c-t)\right]}\right] \\ &\times\frac{3}{8}\chi^{(3)}E_p^2\sum_{\Delta m=1}^{m_p-1}\frac{(\omega_{m_s}\omega_{m_i})^{1/2}}{n(\omega_{m_s})n(\omega_{m_i})}\int d\Omega\frac{S_{si}(\Omega,-\Omega)}{\left(\frac{\gamma_s}{2}-i\Omega\right)\left(\frac{\gamma_i}{2}+i\Omega\right)} \\ &\times a^\dagger(\omega_p+\Delta m\Delta\omega+\Omega)a^\dagger(\omega_p-\Delta m\Delta\omega-\Omega)\,|0\rangle. \end{aligned}$$

Outside of the cavity, the signal and the idler field modes can be spatially separated by filtering. The commutation relations applicable between the fields then lead to the following:

$$\begin{aligned} &a_s(\omega_p+\Omega')\, a_i(\omega_p+\Omega'') \\ &\quad\times a^\dagger(\omega_p+\Delta m\Delta\omega+\Omega)a^\dagger(\omega_p-\Delta m\Delta\omega-\Omega)\,|0\rangle \\ &\quad=\delta(\Omega'-\Omega-\Delta m\Delta\omega)\,\delta(\Omega''+\Omega+\Delta m\Delta\omega)\,|0\rangle. \end{aligned}$$

With these approximations, we obtain

$$\begin{aligned} E_{Out_s}^{(+)}(x,t+\tau)\, E_{Out_i}^{(+)}(x,t)\,|\psi\rangle &\propto e^{i\left[2\omega_p(x/c-t)-\omega_p\tau)\right]} \\ &\times\sum_{\Delta m=1}^{m_p-1}\frac{(\omega_{m_s}\omega_{m_i})^{1/2}}{n(\omega_{m_s})n(\omega_{m_i})}e^{-i\Delta m\Delta\omega\tau} \\ &\times\int d\Omega e^{-i\Omega\tau} \\ &\times\frac{S_{si}(\Omega,-\Omega)}{\left(\frac{\gamma_s}{2}-i\Omega\right)\left(\frac{\gamma_i}{2}+i\Omega\right)}\,|0\rangle. \end{aligned} \tag{21}$$

To find out the signal-idler cross-correlations, we need to calculate the squared module of this vector state. For a first evaluation of this expression, we make further assumptions:

- $\frac{(\omega_{m_s}\omega_{m_i})^{1/2}}{n(\omega_{m_s})n(\omega_{m_i})} \approx \frac{(\omega_p\omega_p)^{1/2}}{n(\omega_p)n(\omega_p)} = \text{const}$,
- $S_{si}(\Omega,-\Omega)\approx 1$ (straightforward when $m_s = m_i$, refer to Sec. 2 of Appendix D).

After the constants have been removed from expression (21), the vector state can be simplified as follows:

$$\begin{aligned} &E_{Out_s}^{(+)}(x,t+\tau)\, E_{Out_i}^{(+)}(x,t)\,|\psi\rangle \\ &\propto e^{i\left[2\omega_p(x/c-t)-\omega_p\tau)\right]}\sum_{\Delta m=1}^{m_p-1}e^{-i\Delta m\Delta\omega\tau}\int\frac{d\Omega e^{-i\Omega\tau}}{\left(\frac{\gamma}{2}\right)^2+\Omega^2}\,|0\rangle. \end{aligned}$$

Then, we replace the integral by its value $2\pi e^{-\frac{\gamma}{2}|\tau|}/\gamma$ and obtain

$$\begin{aligned} &E_{Out_s}^{(+)}(x,t+\tau)\, E_{Out_i}^{(+)}(x,t)\,|\psi\rangle \\ &\propto e^{i\left[2\omega_p(x/c-t)-\omega_p\tau)\right]}e^{-\frac{\gamma}{2}|\tau|}\sum_{\Delta m=1}^{m_p-1}e^{-i\Delta m\Delta\omega\tau}\,|0\rangle. \end{aligned}$$

Finally, the squared modulus of this expression gives us the signal-idler cross-correlations of the following form:

$$G_{IS}^{(2)}(\tau)\propto e^{-\gamma|\tau|}\left|\sum_{\Delta m=1}^{m_p-1}e^{-i\Delta m\Delta\omega\tau}\right|^2. \tag{22}$$

A plot of the $G_{IS}^{(2)}(\tau)$ function is shown in Fig. 4. In our example, as already mentioned, the sum contains in fact only four terms ($m_s = 16,..,19$ and $m_i = 11,..,15$). This figure shows that the emitted photon pairs go out of the cavity at the same time ($\tau = 0$) or that one of the two emitted photons goes out later, after one or multiple round-trips (of time T) in the resonant cavity. A proportion of the photons that resonate in the cavity are lost so that the peaks decrease with the cavity damping rate γ. Otherwise, this graph is similar to the one obtained for an optical parametric oscillator.[27]

We have not performed the calculations in the case where the spectral walk-off is not compensated, but we expect that the spectral walk-off will have an effect similar to an increase of the damping rate of the cavity. This means that the decrease of the amplitude with the signal-idler delay will be more pronounced in the cross-correlation rate graph.

VI. CONCLUSION

We have considered the degenerate four wave mixing in a cavity of a regular VCSEL whose characteristics are outlined in Appendix A.

We have calculated the two-photon production rate, the output spectrum of the emitted photons, and the cross-correlation between the signal and idler photons.

The calculation of the production rate has highlighted the significant impact of the dispersion, illustrated by Eq. (17).

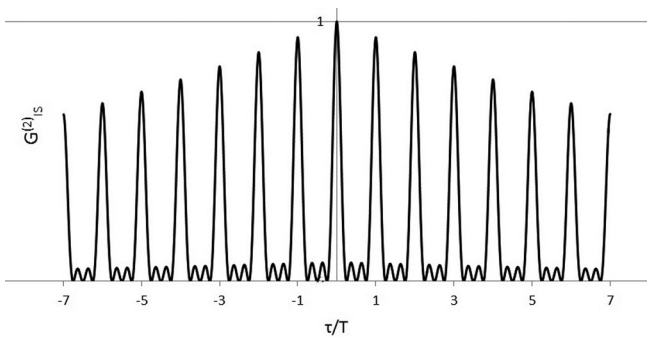

FIG. 4. Normalized signal-idler cross-correlation function $G_{IS}^{(2)}(\tau)$ for $\gamma = 30$ GHz, $\Delta\omega = 3$THz, and $\Delta m = 1,\ldots,4$. The horizontal scale is τ/T, where $T = 2\pi/\Delta\omega$.

This expression shows that the production rate decreases quadratically with the spectral walk-off when the latter is large compared to the cavity damping rate γ.[23]

We have shown that the output spectrum represents a frequency comb as expected. However, in the considered VCSEL, only four modes are being excited below the cavity absorption band. Moreover, the non-compensated spectral walk-off reduces drastically the amplitude of the "teeth" at the sides of the spectrum even within the narrow bandwidth where photon pairs are emitted.

The observed cross-correlations show the highest probability of the simultaneous emission of the signal and idler photons. However, the emission of signal-idler pairs separated by multiples of the period of time necessary for the light to resonate within the cavity has also a non-zero rate. This latter rate decreases when the delay between the emitted signal and idler photons increases.

Despite the relatively low value of the two-photon production rate that we obtained (see Table I), for instance, in comparison to some past experiences,[21,42] we find it worth investigating degenerate four wave mixing in a VCSEL as a potential source of photon pairs. In order to address the key challenge of increasing the production rate, the VCSEL cavity should be

- resonant for the pump and at least one signal and idler modes and, whenever possible, several signal and idler modes,
- with a high value of the third-order non-linear susceptibility $\chi^{(3)}$,
- with a compensation of the spectral walk-off to the maximum possible extent,
- such that it allows a maximum number of signal-idler coupled modes beyond the absorption band,
- such that we can avoid undesirable (for our purpose) effects such as Raman or Brillouin effects and thermo-optical oscillations[43]—in particular, if the pump needs to be stepped up to increase the production rate.

Addressing those challenges may be the subject of a study focused on designing a VCSEL device dedicated to the generation of photon pairs via degenerate four wave mixing.

ACKNOWLEDGMENTS

This work was supported by the Belgian Federal IAP program under Project No. P7/35 Photonics@be. K.P. acknowledges the Methusalem foundation for financial support. E.K. also gratefully acknowledges support from the Brussels Capital Region via the SeCloud project within the Secur'IT strategic platform.

APPENDIX A: THE VCSEL CAVITY UNDER ANALYSIS

In this appendix, we outline the parameters of a realistic VCSEL cavity on which we base our analysis.

We consider a GaAs VCSEL configuration with $Al_{0.25}Ga_{0.75}As/Al_{0.85}Ga_{0.15}As$ distributed Bragg mirrors.[14,15] However, in contrast to the usual VCSEL configuration where the cavity optical thickness is either half or a single wavelength, we consider a much thicker cavity. This allows a design of a VCSEL cavity resonant not only for the pump wavelength but also for the idler and the signal wavelengths as well.

TABLE II. Couples of four wave mixing-generated signal and idler waves in the VCSEL.

Δm	Couple m_s,m_i	λ_s, μm	λ_i, μm	ω_{m_s}, PHz	ω_{m_i}, PHz	Spectral walk-off Δ_{msi}, THz
1	16, 14	0.804	0.903	2.34	2.08	3.4
2	17, 13	0.764	0.964	2.46	1.95	14
3	18, 12	0.729	1.04	2.58	1.81	31
4	19, 11	0.698	1.12	2.69	1.67	54

We assume that the length of the VCSEL cavity is 1.9μm and that the VCSEL cavity is resonant with a pump wave number $m_p = 15$, that is, for a pump wavelength $\lambda_p = 0.850\,\mu$m (wavelengths considered here are "in the vacuum").

Resonant four wave mixing may take place for wave numbers that ensure that the phase matching conditions are met, that is, when $m_s + m_i = 2m_p$. The corresponding resonant wavelengths are then calculated numerically from $2Ln(\lambda_s) = m_s\lambda_s$ and $2Ln(\lambda_i) = m_i\lambda_i$, where $n(\lambda)$ denotes the wavelength-dependent refractive index and L is the length of the VCSEL cavity. Those wavelengths are presented in Table II.

The resonant angular frequencies ω_{m_s} and ω_{m_i} are calculated from those wavelengths: $\omega_{m_s} = 2\pi c/\lambda_s$ and $\omega_{m_i} = 2\pi c/\lambda_i$, where c is the speed of light in the vacuum.

The spectral walk-offs presented in Table II are calculated by considering only the dispersion characterizing the semiconductor materials.

The table shows only four couples of wavelengths because the signal photons of lower wavelengths fall in the absorption band, defined by the wavelength $\lambda = 0.69\mu$m.

For the VCSEL presented in the table, the values for the free spectral range $\Delta\omega$ vary from 115 THz to 139 THz.

We note that the spectral walk-offs Δ_{msi} are significantly larger than the damping coefficient γ_s, for each of the resonant angular frequencies considered in the table. In order to optimize or even allow four wave mixing at a reasonable rate, it will be important to analyze whether the spectral walk-off can be reduced below the cavity damping rate, that is, reduced to a value comparable to γ.[22]

APPENDIX B: INTERACTION HAMILTONIAN

In this appendix, we derive Eq. (7) for the interaction Hamiltonian in three steps.

1. Step 1: assumption on the form of the interaction Hamiltonian

We make the assumption that the interaction Hamiltonian operator in our VCSEL cavity may be approximated by an expression of the following form:[25,43,44]

$$H_{int} = \sum_{s,i}^{\infty} \hbar g a_0^2 a_s^\dagger a_i^\dagger + H.c.\,, \tag{B1}$$

where $a_s^\dagger$ and $a_i^\dagger$ are the creation operators for the signal and idler fields, respectively, a_0 is the amplitude of the pump field, and g is a real coupling constant that must be determined taking into account the physical configuration of the VCSEL cavity.

This simplified form of the interaction Hamiltonian implicitly neglects the self-phase and the cross-phase modulations effects.[43] The only Kerr effect considered here is the four wave mixing.

The sum in Eq. (B1) is performed on all possible couples of signal (s) and idler (i) resonant modes that fulfill energy and momentum conservation requirements.

2. Step 2: correspondence with classical expression

We make a correspondence between the expression that describes the time evolution of the quantized signal mode operator a_s and the classical coupled-mode equations.

The time evolution of the signal mode operator a_s can be written as[43]

$$\frac{da_s}{dt} = \frac{1}{i\hbar}[a_s, H_{tot}] - \frac{\gamma_s}{2}a_s + \sqrt{\gamma_s}V_s,$$

where V_s is the quantum noise operator[43] that avoids a violation of the Heisenberg uncertainty principle.

Taking into account that $H_{tot} = H_{pump} + H_s + H_i + H_{int}$, where H_{pump}, H_s, and H_i denote the respective energy operators of the non-interacting pump, signal, and idler fields, we can conclude that the only term of $[a_s, H_{tot}]$ that includes the operator $a_i^\dagger$ is

$$[a_s, H_{int}] = \hbar g a_0^2 a_i^\dagger.$$

The time evolution of the signal mode operator can then be written as follows:

$$\frac{da_s}{dt} = -ig a_0^2 a_i^\dagger - i\omega_s a_s - \frac{\gamma_s}{2}a_s + \sqrt{\gamma_s}V_s. \tag{B2}$$

In order to determine the value of g, we make a correspondence between this quantum expression and the classical coupled-mode equation for the signal mode derived by Ramirez *et al.*[45] [Eq. (2)]

$$\dot{a}_s = \left[i\omega_s(1 - \alpha_{s0}|\tilde{a}_0|^2 - \alpha_{ss}|a_s|^2 - \alpha_{si}|a_i|^2) - \frac{\gamma_s}{2}\right]a_s - i\omega_s\beta_s\tilde{a}_0{}^2 a_i^* + \sqrt{\gamma_s}s_{m,+}, \tag{B3}$$

where $s_{m,+}$ is a loss term, α_{s0}, α_{ss}, and α_{si} are coefficients corresponding to the self-phase and cross-phase modulations, while β_s (see below) characterizes the energy transfer between the modes by four wave mixing. As mentioned above, we assume $\alpha_{s0} = \alpha_{ss} = \alpha_{si} = 0$.

We note that Ramirez *et al.*[45] used a different convention for the sign of the angular frequencies and that the dimensions of the classical vector potential a_j ($j = s, i, 0$) in Eq. (B3) are defined such that $|a_j|^2$ represents the electromagnetic energy of mode j, while the operator a_s in Eq. (B2) has no dimension and obeys the usual bosonic commutation relations.

Making the correspondence between Eqs. (B2) and (B3) and also making the assumption $\omega_s \approx \omega_p$, we obtain the following value for constant g:

$$g = \hbar\omega_p^2\beta_s,$$

where β_s is obtained by Ramirez *et al.*[45] [see Eqs. (6) and (7) therein]

$$\beta_s = \frac{\int_V dV\epsilon_0\chi^{(3)}\left[\left(\bar{E}_p^*\bar{E}_p^*\right)(\bar{E}_s\bar{E}_i) + 2\left(\bar{E}_p^*\bar{E}_s\right)\left(\bar{E}_p^*\bar{E}_i\right)\right]}{16\int_V dV\epsilon|\bar{E}_p|^2\left(\int_V dV\epsilon|\bar{E}_s|^2\int_V dV\epsilon|\bar{E}_i|^2\right)^{1/2}}.$$

We have assumed that the resonant fields are all polarized along a common transverse direction and assumed the following forms for the amplitude of the resonant pump, signal, and idler fields in the VCSEL cavity:

$$\bar{E}_p = E_p \sin\left(m_p\frac{\pi}{L}z\right)\overline{1_x},$$

$$\bar{E}_s = E_s \sin\left(m_s\frac{\pi}{L}z\right)\overline{1_x},$$

$$\bar{E}_i = E_i \sin\left(m_i\frac{\pi}{L}z\right)\overline{1_x},$$

where $\overline{1_x}$ is a unit polarization vector along the x axis, E_p, E_s, and E_i are the real amplitudes of the classical fields, and $m_s + m_i = 2m_p$.

We obtain the coupling constant in the following form:

$$\begin{aligned} g &= \frac{3\hbar\omega_p^2\epsilon_0\chi^{(3)}}{16\epsilon_0^2 n_p^4 A^2\left(\frac{L}{2}\right)\left(\frac{L}{2}\right)^{1/2}\left(\frac{L}{2}\right)^{1/2}}\int_V dV \sin^2\left(m_p\frac{\pi}{L}z\right) \\ &\quad\times \sin\left((m_s)\frac{\pi}{L}z\right)\sin\left((m_i)\frac{\pi}{L}z\right) \\ &= \frac{3}{32}\frac{\hbar\omega_p^2\chi^{(3)}}{\epsilon_0 n_p^4 V}. \end{aligned} \tag{B4}$$

Note that the units of the coupling coefficient g are s^{-1} and that the integral in expression (B4) is equal to 0 if $m_s + m_i \neq 2m_p$, implying that no energy transfer is possible between modes that do not conserve momentum.

3. Step 3: interaction Hamiltonian as a function of the electric fields

Finally, we express the interaction Hamiltonian as a function of the electric fields in the cavity. In an arbitrary volume, the interaction Hamiltonian may be written as

$$H_{int} = C\varepsilon_0\int_V \chi^{(3)}E_p^{(+)}E_p^{(+)}E_s^{(-)}E_i^{(-)}dV + H.c., \tag{B5}$$

where C is a constant to be determined.

Comparing expressions (B1) and (B5) at time $t = 0$ and requiring momentum conservation, we find $C = 3/2$. Then, the final expression for the interaction Hamiltonian as a function of the electric field operators is

$$H_{int} = \frac{3}{2}\varepsilon_0\int_V \chi^{(3)}E_p^{(+)}E_p^{(+)}E_s^{(-)}E_i^{(-)}dV + H.c. \tag{B6}$$

APPENDIX C: COMPARISON WITH THE PRODUCTION RATE DERIVED FROM QUANTUM FLUCTUATIONS

In this appendix, we compare our results for the two-photon production rate with the results obtained by Chembo[43] from the Heisenberg-Langevin equations. Although the calculation in this article[43] is dedicated to four wave mixing in a whispering-gallery mode resonator, the development may apply as such to a VCSEL cavity if we use the coupling coefficient in the Hamiltonian and the damping factor that corresponds to our physical configuration. Interestingly, this article also presents and calculates a four wave mixing threshold photon number that separates the spontaneous emission of two photons (below threshold) from the stimulated emission of two photons (above threshold).

The following variables were used in Ref. 43:

- $|A_0|^2$ is the photon number at the pump frequency in the cavity,
- $g_0 = n_2 c\hbar\omega_p^2/n_p^2 V$ is the four wave mixing gain (dimension s^{-1}) at the pump frequency, where n_2 is the Kerr coefficient (dimension m^2/W).

Let us emphasize that g_0 is related to the physical configuration of the chosen resonator.[43] Constant g_0 is related to the value of g (B4) for our VCSEL cavity as follows: $g = g_0/8$. When making this comparison, we assume that the interaction Hamiltonian used in Ref. 43 is actually $H_{int} = \hbar g_0 a_0^2 a_s^\dagger a_i^\dagger + H.c.$ instead of $\hbar g_0 a_0^2 a_s^\dagger a_i^\dagger/2 + H.c.$ as described by Chembo[43] in expression (85).

Chembo[43] provided the following expression for the four wave mixing threshold photon number:

$$|A_{th}|^2 = \frac{\gamma_s}{2g_0},$$

and the production rate of the spontaneously emitted photons for a given signal mode m_s:

$$R(m_s) = \rho\frac{\gamma_s}{2}\frac{g_0^2|A_0|^4}{\left(\frac{\gamma_s}{2}\right)^2 - g_0^2|A_0|^4 + \xi_{m_s}^2}, \tag{C1}$$

where ρ is the ratio between the outcoupling and the total losses and ξ_{m_s} is described as the overall shift induced by laser detuning, group-velocity dispersion, and self-phase modulation for mode m_s.

We take $\rho = 1$, that is, we assume that the production rate of photons represents the only loss in the cavity. We also make the approximation that ξ_{m_s} represents the spectral walk-off between mode m_s and the pump mode.

With the following values,

- $\gamma_s = 300 \times 10^9 \mathrm{s}^{-1}$,
- $n_2 = 3.3 \times 10^{-13} \mathrm{cm}^2/\mathrm{W}$,
- $\omega_p = 2.2 \times 10^{15} \mathrm{s}^{-1}$,
- $n_p = 3.4$,
- $V = 1.87\,\mu\mathrm{m} \times \pi(2\,\mu\mathrm{m})^2 = 2.3 \times 10^{-17}\mathrm{m}^3$,

we obtain a four wave mixing threshold photon number $|A_{th}|^2 = 8.4 \times 10^6$. This corresponds to the following four wave mixing threshold for the classical pump electric field travelling in the positive x direction in the cavity

$$E_{p_{th}} = \frac{1}{2}\left(\frac{\hbar\omega_p}{\varepsilon_0 n_p^2 V}\right)^{1/2}|A_{th}| = 1.4 \times 10^7 \mathrm{V/m}.$$

The corresponding maximum of the pump electric field standing wave in the cavity amounts for $4E_{p_{th}} = 5.6 \times 10^7 \mathrm{V/m}$.

We evaluate the production rate of the spontaneously emitted photons for the mode $m_s = 16$ when the cavity is pumped below the four wave mixing threshold ($|A_0|^2 \ll \gamma_s/2g_0$) in the following two cases.

1. Production rate with compensation of the spectral walk-off

In the case $\xi_{m_s} = 0$, the production rate is mode-independent. Replacing g_0 by g in (C1), we recover the production rate (15) calculated by the perturbative method in the case $\gamma_s = \gamma_i$:

$$R \approx \frac{2g^2|A_0|^4}{\gamma_s} \approx \frac{2}{\gamma_s}\left(\frac{3\chi^{(3)}\omega_p E_p^2}{8n_p^2}\right)^2. \tag{C2}$$

2. Production rate with no compensation of the spectral walk-off

When the spectral walk-off is significantly larger than the damping coefficient $\Delta_{msi} \gg \gamma_s$, we recover the production rate (17) by making the approximation

$$R(m_s) \approx \gamma_s\frac{g^2|A_0|^4}{2\xi_{m_s}^2} \approx \frac{\gamma_s}{2}\left(\frac{3\chi^{(3)}\omega_p E_p^2}{4n_p^2\Delta_{msi}}\right)^2,$$

where we have used $\xi_{m_s} = \Delta_{msi}/2$ to take into account that the spectral walk-off Δ_{msi} derived in Appendix A is taken between the signal and idler, while numbers in (C1) refer to the spectral walk-off between signal and pump waves.

APPENDIX D: VALIDATION OF SOME ASSUMPTIONS

1. Large Δt approximation

In Sec. III A, we have assumed that Δt was sufficiently large to perform the following approximation:

$$\begin{aligned}
&\int_{-\infty}^{+\infty} d\Omega' \frac{\mathrm{sinc}^2\left[\left(2k_p(\omega_p) - k_s(\Omega) - k_i(\Omega')\right)\frac{L}{2}\right]}{\left[\left(\frac{\gamma_s}{2}\right)^2 + \Omega^2\right]\left[\left(\frac{\gamma_i}{2}\right)^2 + \Omega'^2\right]} \\
&\quad\times \mathrm{sinc}^2\left[(\Omega + \Omega' - \Delta_{msi})\frac{\Delta t}{2}\right] \\
&\approx \frac{\mathrm{sinc}^2\left[\left(2k_p(\omega_p) - k_s(\Omega) - k_i(\Delta_{msi} - \Omega)\right)\frac{L}{2}\right]}{\left[\left(\frac{\gamma_s}{2}\right)^2 + \Omega^2\right]\left[\left(\frac{\gamma_i}{2}\right)^2 + (\Delta_{msi} - \Omega)^2\right]} \\
&\quad\times \int_{-\infty}^{+\infty} d\Omega' \mathrm{sinc}^2\left[(\Omega + \Omega' - \Delta_{msi})\frac{\Delta t}{2}\right]
\end{aligned} \tag{D1}$$

for all values of Ω, considered here as a parameter. We can now replace the factor $\mathrm{sinc}^2[(2k_p(\omega_p) - k_s(\Omega) - k_i(\Omega'))\frac{L}{2}]$ in (D1) by its value calculated in $\Omega' = \Delta_{msi} - \Omega$ because it is a slowly varying function of Ω' in comparison to the two other factors.

In Sec. 2 of Appendix D, we show that the value of $\mathrm{sinc}^2[(2k_p(\omega_p) - k_s(\Omega) - k_i(\Delta_{msi} - \Omega))\frac{L}{2}]$ can safely be approximated by 1 for all relevant values of Ω when $m_s = m_i$, which is applicable in this case. This means that validating the approximation (D1) is equivalent to proving that

$$\int_{-\infty}^{+\infty} d\Omega' \frac{\mathrm{sinc}^2\left[(\Omega + \Omega' - \Delta_{msi})\frac{\Delta t}{2}\right]}{\left[\left(\frac{\gamma_i}{2}\right)^2 + \Omega'^2\right]} \approx \frac{1}{\left[\left(\frac{\gamma_i}{2}\right)^2 + (\Delta_{msi} - \Omega)^2\right]} \times \int_{-\infty}^{+\infty} d\Omega' \mathrm{sinc}^2\left[(\Omega + \Omega' - \Delta_{msi})\frac{\Delta t}{2}\right].$$

The most defavorable case for the assumption under validation is when the sinc^2 function is centered in the interval where $((\frac{\gamma_i}{2})^2 + \Omega'^2)^{-1}$ varies the fastest, that is, when the sinc^2 function is centered on $\Omega' = \gamma_i/2\sqrt{3}$.

With $\gamma_i = 300\,\mathrm{GHz}$, when numerically computing the value of the integral

$$\int_{-\infty}^{+\infty} d\Omega' \frac{\mathrm{sinc}^2\left[\left(\Omega' - \gamma_i/2\sqrt{3}\right)\frac{\Delta t}{2}\right]}{\left[\left(\frac{\gamma_i}{2}\right)^2 + \Omega'^2\right]},$$

one finds that the approximation described by (D1) results in a relative error on the integral of 3×10^{-4} for a value of $\Delta t = 10^{-8}$s and a relative error on the integral of 3×10^{-3} when $\Delta t = 10^{-9}$s.

For $\gamma_i = 300\,\mathrm{GHz}$, we will consider that the approximation is valid as soon as $\Delta t \geq 10^{-8}$s.

2. Approximate value of $\mathrm{sinc}^2[(2k_p(\omega_p) - k_s(\Omega) - k_i(\Delta_{msi} - \Omega))\frac{L}{2}]$

The value $|S_{si}(\Omega, \Delta_{msi} - \Omega)|^2$ where $S_{si}(\Omega, \Omega')$ is defined by Eq. (10) appears in a number of equations, multiplied by a Lorentzian centered on $\Omega = 0$ and integrated from $\Omega = -\infty$ to $\Omega = +\infty$ [such as in Eq. (13) where $\Delta_{msi} = 0$]. In those cases, it is approximated by 1 when $m_s = m_i$.

We validate this approximation in the case of the VCSEL described in Appendix A. We first note that the argument of the sinc function is 0 when $\Omega = 0$ (because $k_s(0)$ and $k_i(\Delta_{msi})$ are resonant modes that ensure phase matching when $m_s = m_i$). We then try to evaluate the maximum value that the argument of the sinc function can take for non-zero values of Ω in the case where $\Omega \leq \gamma_s$, where γ_s is the full width at half maximum of the Lorentzian.

The dispersion in the cavity is the highest at high frequencies, and we calculate the argument of the sinc function in the region $m_s = m_i = 4$ for $\Omega = \gamma_s$.

$$\begin{aligned}&\left(2k_p(\omega_p) - k_s(\Omega) - k_i(\Delta_{msi} - \Omega)\right)\frac{L}{2} \\ &\approx \left(2k_p(\omega_p) - k_s(0) - k_i(0) - \Omega\frac{\partial k_s}{\partial \Omega} + \Omega\frac{\partial k_i}{\partial \Omega}\right)\frac{L}{2} \\ &\approx \Omega\left(\frac{\partial k_i}{\partial \Omega} - \frac{\partial k_s}{\partial \Omega}\right)\Big|_{\Omega=0}\frac{L}{2} \approx \Omega\left(\frac{\partial k}{\partial \omega}\Big|_{\omega=\omega_{m_i}} - \frac{\partial k}{\partial \omega}\Big|_{\omega=\omega_{m_s}}\right)\frac{L}{2}.\end{aligned}$$

For our VCSEL, we calculate numerically that $\frac{\partial k}{\partial \omega}|_{\omega=\omega_{m_i}} < \frac{\partial k}{\partial \omega}|_{\omega=\omega_{m_s}}$. Both values have the same sign, and we can write

$$\begin{aligned}&|2k_p(\omega_p) - k_s(\gamma_s) - k_i(-\gamma_s)|\frac{L}{2} \\ &\leq \gamma_s\left|\frac{\partial \mathrm{k}}{\partial \omega}\Big|_{\omega=\omega_{m_s}}\right|\frac{L}{2} \leq \gamma_s\left|\frac{\omega_{m_s}}{c}\frac{\partial n}{\partial \omega}\Big|_{\omega=\omega_{m_s}} + \frac{n(\omega_{m_s})}{c}\right|\frac{L}{2}.\end{aligned}$$

For $\omega_{m_s} = 2.69 \times 10^{15}\mathrm{s}^{-1}$, we obtain numerically

$$\frac{\partial n}{\partial \omega}\Big|_{\omega=\omega_{m_s}} \approx 3 \times 10^{-16}\mathrm{s} \quad \text{and}$$

$$|2k_p(\omega_p) - k_s(\gamma_s) - k_i(\Delta_{msi} - \gamma_s)|\frac{L}{2} \leq 0.0016.$$

This validates the approximation

$$|S_{si}(\Omega, \Delta_{msi} - \Omega)|^2 = \mathrm{sinc}^2\left[\left(2k_p(\omega_p) - k_s(\Omega) - k_i(\Delta_{msi} - \Omega)\right)\frac{L}{2}\right] \approx 1$$

for relevant values of Ω (that is, $\Omega \leq \gamma_s$) when $m_s = m_i$.

3. Validity of perturbative treatment

The assumption $\Delta t \geq 10^{-8}$s obtained in the large Δt approximation in Sec. 1 of Appendix D combined with the assumptions allowing a perturbative treatment, which were $\Delta t \ll \Delta t/\langle\psi|\psi\rangle$ and $\langle\psi|\psi\rangle/\Delta t \ll \gamma_{s/i}$, results in a limited range of acceptable values for the calculated two-photon production rate. The values obtained for the two-photon production rate, in the range of $10^{-5} < \langle\psi|\psi\rangle/\Delta t < 3 \times 10^5$ with $\gamma_s = \gamma_i = 300\,\mathrm{GHz}$ (see Table I), are compatible with all the assumptions.

[1]G. J. Milburn, E. Knill, and R. Laflamme, "A scheme for efficient quantum computation with linear optics," Nature **409**, 46–52 (2001).
[2]J. D. Franson, M. M. Donegan, M. J. Fitch, B. C. Jacobs, and T. B. Pittman, "High-fidelity quantum logic operations using linear optical elements," Phys. Rev. Lett. **89**, 137901 (2002).
[3]C. H. Bennett, G. Brassard, C. Crépeau, R. Jozsa, A. Peres, and W. K. Wootters, "Teleporting an unknown quantum state via dual classical and Einstein-Podolsky-Rosen channels," Phys. Rev. Lett. **70**, 1895–1899 (1993).
[4]E. Lombardi, F. Sciarrino, S. Popescu, and F. De Martini, "Teleportation of a vacuum̆one-photon qubit," Phys. Rev. Lett. **88**, 070402 (2002).
[5]G. B. C. H. Bennett, "Quantum cryptography: Public key distribution and coin tossing," in *Proceedings of the IEEE International Conference on Computers, Systems and Signal Processing* (1984), pp. 175–179.

[6]A. K. Ekert, "Quantum cryptography based on bell's theorem," Phys. Rev. Lett. **67**, 661–663 (1991).
[7]C. H. Bennett, F. Bessette, G. Brassard, L. Salvail, and J. Smolin, "Experimental quantum cryptography," J. Cryptol. **5**, 3–28 (1992).
[8]K. R. Motes, J. P. Olson, E. J. Rabeaux, J. P. Dowling, S. J. Olson, and P. P. Rohde, "Linear optical quantum metrology with single photons: Exploiting spontaneously generated entanglement to beat the shot-noise limit," Phys. Rev. Lett. **114**, 170802 (2015).
[9]P. G. Kwiat, E. Waks, A. G. White, I. Appelbaum, and P. H. Eberhard, "Ultrabright source of polarization-entangled photons," Phys. Rev. A **60**, R773–R776 (1999).
[10]K. Zielnicki, K. Garay-Palmett, R. Dirks, A. B. U'Ren, and P. G. Kwiat, "Engineering of near-IR photon pairs to be factorable in space-time and entangled in polarization," Opt. Express **23**, 7894–7907 (2015).
[11]D. C. Unitt, A. J. Bennett, P. Atkinson, K. Cooper, P. See, D. Gevaux, M. B. Ward, R. M. Stevenson, D. A. Ritchie, and A. J. Shields, "Quantum dots as single-photon sources for quantum information processing," J. Opt. B: Quantum Semiclassical Opt. **7**, S129–S134 (2005).
[12]X. Ding, Y. He, Z.-C. Duan, N. Gregersen, M.-C. Chen, S. Unsleber, S. Maier, C. Schneider, M. Kamp, S. Höfling, C.-Y. Lu, and J.-W. Pan, "On-demand single photons with high extraction efficiency and near-unity indistinguishability from a resonantly driven quantum dot in a micropillar," Phys. Rev. Lett. **116**, 020401 (2016).
[13]A. Crespi, R. Osellame, R. Ramponi, D. J. Brod, E. F. Galvo, N. Spagnolo, C. Vitelli, E. Maiorino, P. Mataloni, and F. Sciarrino, "Integrated multimode interferometers with arbitrary designs for photonic boson sampling," Nat. Photonics **7**, 545–549 (2013).
[14]K. Iga, "Surface-emitting laser—Its birth and generation of new optoelectronics field," IEEE J. Sel. Top. Quantum Electron. **6**, 1201–1215 (2000).
[15]R. Michalzik SpringerLink, *VCSELs: Fundamentals, Technology and Applications of Vertical-Cavity Surface-Emitting Lasers* (Springer, Berlin/Heidelberg, 2013), Vol. 166.
[16]M. Grabherr, "New applications boost vcsel quantities: Recent developments at Philips," Proc. SPIE **9381**, 938102 (2015).
[17]D. Francis, W. Yuen, H. Chen, G. Li, and C. Chang-Hasnain, "Monolithic 2d-vcsel array with ¿2 w cw and ¿5 w pulsed output power," Electron. Lett. **34**, 2132 (1998).
[18]M. Miller, M. Grabherr, R. Jger, and K. J. Ebeling, "High-power vcsel arrays for emission in the watt regime at room temperature," IEEE Photonics Technol. Lett. **13**, 173–175 (2001).
[19]E. Bosman, J. Missinne, B. V. Hoe, G. V. Steenberge, S. Kalathimekkad, J. V. Erps, I. Milenkov, K. Panajotov, T. V. Gijseghem, P. Dubruel, H. Thienpont, and P. V. Daele, "Ultrathin optoelectronic device packaging in flexible carriers," IEEE J. Sel. Top. Quantum Electron. **17**, 617–628 (2011).
[20]M.-C. Amann and W. Hofmann, "Inp-based long-wavelength vcsels and vcsel arrays," IEEE J. Sel. Top. Quantum Electron. **15**, 861–868 (2009).
[21]S. Clemmen, K. P. Huy, W. Bogaerts, R. G. Baets, P. Emplit, and S. Massar, "Continuous wave photon pair generation in silicon-on-insulator waveguides and ring resonators," Opt. Express **17**, 16558–16570 (2009).
[22]R. M. Camacho, "Entangled photon generation using four-wave mixing in azimuthally symmetric microresonators," Opt. Express **20**, 21977–21991 (2012).
[23]J. Chen, Z. H. Levine, J. Fan, and A. L. Migdall, "Frequency-bin entangled comb of photon pairs from a silicon-on-insulator micro-resonator," Opt. Express **19**, 1470–1483 (2011).
[24]U. Herzog, M. Scholz, and O. Benson, "Theory of biphoton generation in a single-resonant optical parametric oscillator far below threshold," Phys. Rev. A **77**, 023826 (2008).
[25]J. Chen, X. Li, and P. Kumar, "Two-photon-state generation via four-wave mixing in optical fibers," Phys. Rev. A **72**, 033801 (2005).
[26]D. Walls and G. Milburn, *Quantum Optics* (Springer, 2008).
[27]M. Scholz, L. Koch, and O. Benson, "Analytical treatment of spectral properties and signal-idler intensity correlations for a double-resonant optical parametric oscillator far below threshold," Opt. Commun. **282**, 3518–3523 (2009).
[28]R. Boyd and G. Fischer, "Nonlinear optical materials," in *Encyclopedia of Materials: Science and Technology*, 2nd ed., edited by K. J. Buschow, W. C. Chang, and F. I. J. K. M. Veyssire (Elsevier, Oxford, 2001), pp. 6237–6244.
[29]R. Michalzik and K. J. Ebeling, "Generalized bv diagrams for higher order transverse modes in planar vertical-cavity laser diodes," IEEE J. Quantum Electron. **31**, 1371–1379 (1995).
[30]H. Wenzel and H.-J. Wnsche, "The effective frequency method in the analysis of vertical-cavity surface-emitting lasers," IEEE J. Quantum Electron. **33**, 1156–1162 (1997).
[31]M. J. Noble, J. A. Lott, and J. P. Loehr, "Quasi-exact optical analysis of oxide-apertured microcavity vcsel's using vector finite elements," IEEE J. Quantum Electron. **34**, 2327–2339 (1998).
[32]M. Dems, T. Czyszanowski, and K. Panajotov, "Numerical analysis of high q-factor photonic-crystal vcsels with plane-wave admittance method," Opt. Quantum Electron. **39**, 419–426 (2007).
[33]T. Czyszanowski, M. Dems, and K. Panajotov, "Impact of the hole depth on the modal behaviour of long wavelength photonic crystal vcsels," J. Phys. D: Appl. Phys. **40**, 2732–2735 (2007).
[34]D. F. Siriani, P. O. Leisher, and K. D. Choquette, "Loss-induced confinement in photonic crystal vertical-cavity surface-emitting lasers," IEEE J. Quantum Electron. **45**, 762–768 (2009).
[35]M. Dems, I.-S. Chung, P. Nyakas, S. Bischoff, and K. Panajotov, "Numerical methods for modeling photonic-crystal vcsels," Opt. Express **18**, 16042–16054 (2010).
[36]T. Czyszanowski, M. Dems, and K. Panajotov, "Single mode condition and modes discrimination in photonic-crystal 1.3 μm alingaas/inp vcsel," Opt. Express **15**, 5604–5609 (2007).
[37]K. Panajotov, M. Sciamanna, M. A. Arteaga, and H. Thienpont, "Optical feedback in vertical-cavity surface-emitting lasers," IEEE J. Sel. Top. Quantum Electron. **19**(4), 1700312 (2013).
[38]J. Tignon, J. Bloch, C. Diederichs, C. Delalande, G. Dasbach, A. Lematre, C. Ciuti, and P. Roussignol, "Parametric oscillation in vertical triple microcavities," Nature **440**, 904–907 (2006).
[39]R. P. Stanley, R. Houdr, U. Oesterle, M. Ilegems, and C. Weisbuch, "Coupled semiconductor microcavities," Appl. Phys. Lett. **65**, 2093–2095 (1994).
[40]K. Panajotov, M. Zujewski, and H. Thienpont, "Coupled-cavity surface-emitting lasers: Spectral and polarization threshold characteristics and electrooptic switching," Opt. Express **18**, 27525–27533 (2010).
[41]D. S. Chemla and D. A. B. Miller, "Room-temperature excitonic nonlinear-optical effects in semiconductor quantum-well structures," J. Opt. Soc. Am. B **2**, 1155–1173 (1985).
[42]U. Herzog, M. Scholz, F. Wolfgramm, and O. Benson, "Narrow-band single photons from a single-resonant optical parametric oscillator far below threshold," Appl. Phys. Lett. **91**, 191104 (2007).
[43]Y. K. Chembo, "Quantum dynamics of Kerr optical frequency combs below and above threshold: Spontaneous four-wave mixing, entanglement, and squeezed states of light," Phys. Rev. A **93**, 033820 (2016).
[44]L. Mandel and E. Wolf, *Optical Coherence and Quantum Optics* (Cambridge University Press, Cambridge/New York, 1995).
[45]D. M. Ramirez, A. W. Rodriguez, H. Hashemi, J. D. Joannopoulos, M. Soljačić, and S. G. Johnson, "Degenerate four-wave mixing in triply resonant kerr cavities," Phys. Rev. A **83**, 033834 (2011).